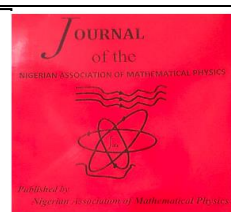


# The Nigerian Association of Mathematical Physics

Journal homepage: <https://nampjournals.org.ng>



## MONTE CARLO SIMULATIONS OF ION BOMBARDMENT AND CALCULATION OF THE ION RANGE AND SPUTTER YIELD OF CAESIUM MIXED-HALIDE DOUBLE PEROVSKITES

\*Oyeleye, M. O and Oyewande, O. E.

\*Department of Physical Sciences, Crescent University Abeokuta

Department of Physics, University of Ibadan.

### ARTICLE INFO

#### Article history:

Received xxxxx

Revised xxxxx

Accepted xxxxx

Available online xxxxx

#### Keywords:

Perovskites,  
Ion beam  
sputtering,  
Power  
conversion  
efficiency,  
Photovoltaic  
applications,  
Monte Carlo  
simulation  
software.

### ABSTRACT

*This paper investigates the sputtering behaviour of selected double perovskites under ion bombardment, aiming to determine the sputtering angle for maximum yield and projected range. It follows up a new approach for the estimation of the power conversion efficiency of single perovskite materials from their sputtering and explores whether double perovskites exhibit similar angular characteristics as single perovskites, with respect to ion range and sputter yield. This research presents the projected ranges and sputter yields for various ions impacting caesium-sodium-indium halide double perovskites,  $Cs_2NaInX_6$  [ $X = Br, I, Cl$ ]. Findings such as Sputter yield and Ion range indicate potential applications in solar energy, contributing to the understanding of ion sputtering mechanisms and advancing the fabrication of efficient thin-film photovoltaic devices. This research has similar sputter characteristics as the single perovskites exhibiting a maximum yield at angle of incidence of  $78^\circ$*

### 1. INTRODUCTION

Metal halide perovskites have emerged as front-runners in the development of next-generation optoelectronic devices due to their exceptional charge transport properties, defect tolerance, and low-cost fabrication processes. However, the most widely studied perovskite is based on lead, such as methylammonium lead iodide ( $CH_3NH_3PbI_3$ ) suffer from serious drawbacks including toxicity and instability under environmental exposure [11]. These concerns have led to an intensive global search for lead-free alternatives, with particular focus on double perovskites, which offer greater compositional flexibility and improved environmental stability [15,18]. Extensive studies on improving these perovskite materials have extrapolated into developing double perovskites with  $A_2BB'X_6$  stoichiometry [2].

\*Corresponding author: OYELEYE, M. O.

E-mail address: [oyeleyemujeeb@gmail.com](mailto:oyeleyemujeeb@gmail.com)

<https://doi.org/10.60787/jnamp.vol72no.657>

1118-4388© 2026 JNAMP. All rights reserved

Among these, the cesium-based elpasolite double perovskites,  $\text{Cs}_2\text{BB}'\text{X}_6$  (where B and B' are monovalent and trivalent metal cations, respectively, and X is a halide), have received growing attention. In particular,  $\text{Cs}_2\text{NaInX}_6$  (X = Cl, Br, I) has emerged as a promising lead-free material, combining the structural stability of the double perovskite framework with the benign nature of its constituent elements. These materials exhibit wide and tunable bandgaps, high thermal stability, and potential for diverse applications in radiation detection, photodetectors, and, increasingly, photovoltaics [5,8]. These lead-free double perovskites exhibit tunable optoelectronic properties, environmental safety, and enhanced chemical and thermal stability, making them promising candidates for photovoltaic applications [9].

The tunability of halide composition (Cl, Br, I) in  $\text{Cs}_2\text{NaInX}_6$  significantly influences its optical and electronic properties, such as bandgap energy, ion migration behavior, and defect tolerance [5,18]. While the intrinsic wide bandgap (typically 3.0–4.0 eV depending on halide) presents challenges for solar cell applications, these materials are highly attractive for UV photodetection and tandem solar cell architectures [16]. Moreover, the all-inorganic nature of  $\text{Cs}_2\text{NaInX}_6$  enhances its long-term stability against humidity and thermal stress, making it suitable for harsh environments. To enable scalable device fabrication and better understand these materials under processing or operating conditions, it is crucial to study their interaction with energetic particles, such as ions used in thin-film processing, doping, or space applications.

Ion-beam surface sputtering is a widely employed technique for surface analysis, thin-film deposition, and nanostructuring [1,7,14]. In this process, energetic ions (commonly inert gases such as  $\text{Ar}^+$  or  $\text{Ne}^+$ ) impinge on the target material, triggering collision cascades that result in atomic displacements, sputtering, and defect formation [11,19]. While this approach has been successfully applied to understand sputtering and ion transport in lead and tin-based perovskites [11], similar studies for lead-free double perovskites, especially  $\text{Cs}_2\text{NaInX}_6$ , remain sparse. This gap in literature leaves open questions about the radiation tolerance, sputtering efficiency, and damage behavior of these promising materials. To address this, we apply Monte Carlo simulation techniques specifically the SRIM and TRIM packages developed by Ziegler and Biersack to investigate the ion range and sputter yield of  $\text{Cs}_2\text{NaInX}_6$  compounds. These simulations use a binary collision approximation (BCA) to statistically model the ion-solid interactions, accounting for nuclear stopping, electronic energy loss, and material-specific parameters such as density and stoichiometry [20].

The most suitable group of materials for a case study in this regard are cesium-based double perovskites, particularly  $\text{Cs}_2\text{NaInX}_6$  (X = Cl, Br, I), which are lead-free, inorganic halide perovskites. These materials adopt a double perovskite structure, where the B-site is alternately occupied by monovalent ( $\text{Na}^+$ ) and trivalent ( $\text{In}^{3+}$ ) metal cations in a rock-salt ordering, and the X-site is occupied by halide ions. While  $\text{Cs}_2\text{NaInX}_6$  compounds possess wide bandgaps typically ranging from ~3.0 eV for iodide to ~4.2 eV for chloride they have been identified as structurally stable and environmentally benign candidates for ultraviolet photodetection and radiation detection applications [5,8]. These double perovskites offer flexibility in tuning electronic and structural properties through halide mixing and cation substitution strategies [16].

In this paper, we studied the range and sputter yield of ions in  $\text{Cs}_2\text{NaInCl}_6$ ,  $\text{Cs}_2\text{NaInBr}_6$ , and  $\text{Cs}_2\text{NaInI}_6$  double perovskites under ion bombardment. Monte Carlo simulations were performed using the SRIM (Stopping and Range of Ions in Matter) and TRIM (Transport of Ions in Matter) packages. We used inert gas ions  $\text{Ne}^+$  and  $\text{Ar}^+$  as projectiles in the sputtering process due to their wide use in experimental surface analysis and minimal chemical interaction with the target. The simulations were carried out over varying ion energies (1–10 keV) and incidence angles ( $0^\circ$ – $89^\circ$ ) to provide detailed insight into the projected ion range, energy loss mechanisms, and element-specific sputter yields. This

computational investigation aims to establish a foundational understanding of how different halide constituents (Cl<sup>-</sup>, Br<sup>-</sup>, I<sup>-</sup>) in Cs<sub>2</sub>NaInX<sub>6</sub> influence the ion-matter interaction characteristics and to evaluate the suitability of these double perovskites for applications requiring stability under irradiation or precision in ion-assisted processing.

## THEORETICAL BACKGROUND

Ion sputtering under energetic particle bombardment is fundamentally described by Sigmund's collision cascade theory by Peter Sigmund.

**Ion-beam sputtering as a pattern-forming, non-equilibrium process:** Under ion bombardment, atoms are ejected via collision cascades whose deposited energy density inside the solid is well described by Sigmund's Gaussian model. For an ion of energy  $\epsilon$  penetrating an average depth  $a$ , the local energy deposition at position  $r' = (x, y, z)$  relative to the impact point is:

$$E(r') = \frac{\epsilon}{[(2\pi)^{3/2} \sigma \mu^2]} \exp\left[ \frac{-(z+a)^2}{2\sigma^2} - \frac{x^2+y^2}{2\mu^2} \right] \text{----- (1)}$$

where  $\sigma$  and  $\mu$  are the longitudinal and transverse cascade widths. The local erosion velocity follows from the deposited energy integrated over the "active" near-surface region,

$$v \equiv -\frac{\partial h}{\partial t} = P_m \int_R \Phi(r) E(r) dr \text{----- (2)}$$

with ion flux fraction  $\Phi$  and proportionality constant  $p_m$ . These ingredients underpin both continuum surface-evolution equations and discrete Monte-Carlo models of sputtering [10,13]

**Discrete/Monte-Carlo viewpoint and link to SRIM/TRIM:** In lattice-based Monte-Carlo sputtering models (e.g., HKGK), the surface is a 2D lattice  $h(i,j)$  with periodic boundaries. Erosion at a site occurs with probability  $p_e \propto E(r)$  (Sigmund energy), and surface diffusion is implemented as nearest-neighbour hops with probability  $p_d$ . One Monte-Carlo step comprises an erosion sweep over the energized region followed by a full-lattice diffusion sweep; time is measured in MC steps per site to remove size effects. These models reproduce ripple formation, orientation changes with angle, and the increase of  $\lambda$  with time in extended regimes. This discrete perspective aligns naturally with the BCA-based SRIM/TRIM simulations used for projected ranges and sputter yields: both inherit their physics from the same deposited-energy kernel  $E(r)$  and encode the strong incidence-angle dependence that yields near-grazing-angle maxima [10].

## 2 METHODOLOGY

In this section we provide the specific details of our simulation. Details of the theoretical background for the calculations and simulation algorithms embedded in the TRIM and SRIM packages are discussed in the papers by Ziegler and Biersack [12,17,20]. SRIM was used to perform Monte Carlo simulations of the range of inert gas ions, Ne<sup>+</sup> and Ar<sup>+</sup>, with energies varied from 1 keV to 10 keV, at normal incidence on the targets. Ion energies in sputtering experiments, in general, fall within this range. The ones that do not fall within the range are low-energy sputtering experiments with ion energy around 500 eV. Hence, the chosen range is relevant to typical ion energies. The targets were cesium-based double perovskites Cs<sub>2</sub>NaInCl<sub>6</sub>, Cs<sub>2</sub>NaInBr<sub>6</sub>, and Cs<sub>2</sub>NaInI<sub>6</sub>. While TRIM was used to perform Monte Carlo simulations for the number of each component of the perovskites yielded as a result of bombardment of the perovskite by an incident ion, for varied incidence angles from 0° to 89°, and for ion energies 1 keV and 5 keV. In the TRIM set-up, perovskite wafer thickness of 35 nm was used, the target thickness of 35 nm was selected to ensure that ions with energies up to 10 keV remained fully contained within the simulation domain, thereby minimizing artificial ion transmission effects. Test simulations confirmed that

increasing thickness beyond this value did not significantly alter sputter yield results, indicating convergence with respect to target depth. For both SRIM and TRIM, the  $\text{Cs}_2\text{NaInX}_6$  compounds were built from their components in the stoichiometric ratio 2:1:1:6 for Cs, Na, In, and halide (Cl, Br, or I), respectively. The experimental densities used were  $3.89 \text{ g/cm}^3$  for  $\text{Cs}_2\text{NaInCl}_6$  [8] and  $4.41 \text{ g/cm}^3$  for  $\text{Cs}_2\text{NaInBr}_6$  [5]. For  $\text{Cs}_2\text{NaInI}_6$  where experimental density data were unavailable, density was estimated from compositional scaling relative to  $\text{Cs}_2\text{NaInBr}_6$ . This introduces minor uncertainty in absolute projected range values; however, comparative trends across halide compositions remain valid, a density of  $5.09 \text{ g/cm}^3$  was calculated based on atomic mass and volume scaling from the bromide variant. An amount of 1000 ions was used for each simulation to allow the simulation to run for a reasonably long time, while larger ion counts improve statistical precision, preliminary tests indicated that the relative variation in sputter yield remained within acceptable computational uncertainty for the trends investigated. The results therefore represent statistically stable average values suitable for comparative analysis. The “Monolayer Collision Step/Surface Sputtering” option was selected to calculate the sputter yield in the TRIM set-up, while detailed calculation with full damage cascade was performed to calculate the projected range in the SRIM set-up.

## RESULTS AND DISCUSSION

The results of our simulations are presented and discussed in this section. Similar trends were observed for the two inert gas ions ( $\text{Ne}^+$  and  $\text{Ar}^+$ ), though higher values of projected ion range and lower sputter yield were generally obtained for  $\text{Ne}^+$ , whereas  $\text{Ar}^+$  showed lower ion penetration and higher sputter yield across the studied materials. The simulations were started with the three halide variants of the  $\text{Cs}_2\text{NaInX}_6$  double perovskites, namely  $X = \text{Cl}$ ,  $\text{Br}$ , and  $\text{I}$ . Figure 1 show the results of the projected range of ions in the three perovskites for different ion energies ranging from 1 keV to 10 keV. The values of the linear range of the ions in the different targets were close, especially for sputtering with  $\text{Ar}^+$ . These indicated that the three materials, chloride, bromide, and iodide double perovskites are remarkably similar in terms of their stopping power to energetic ion irradiation. The similarity in their ion range behavior supports the choice of Br and Cl as viable substitutes for I in cesium-based indium halide double perovskites, and this is in agreement with the results obtained by Oyewande and Akinpelu (2018) for Pb- and Sn-based single perovskites.

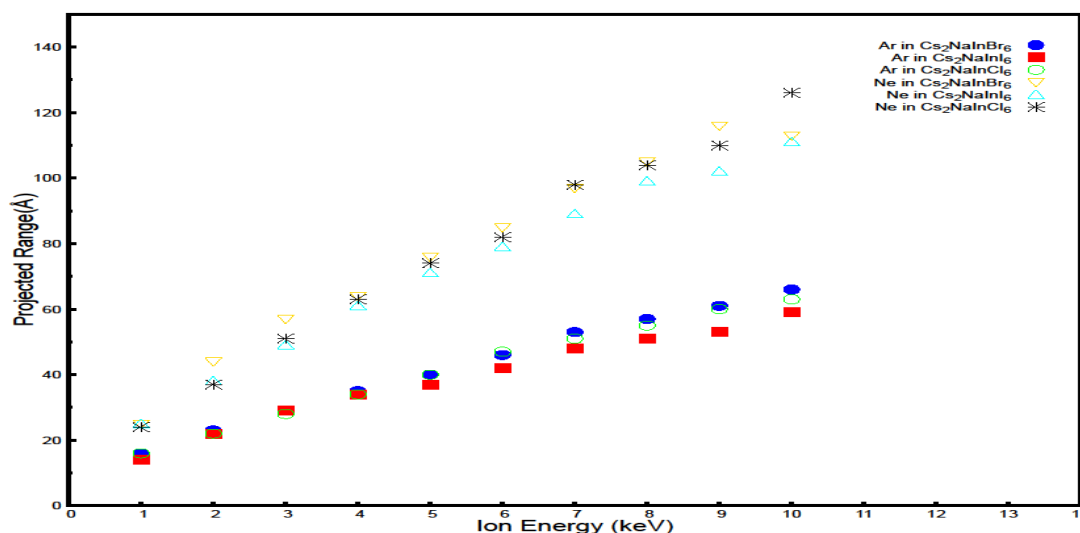


**Fig. 1: Projected Range of  $\text{Ne}^+$  and  $\text{Ar}^+$  in  $\text{Cs}_2\text{NaInCl}_6$ ,  $\text{Cs}_2\text{NaInBr}_6$ , and  $\text{Cs}_2\text{NaInI}_6$  double perovskites target for different ion energies from 1keV to 10keV.**

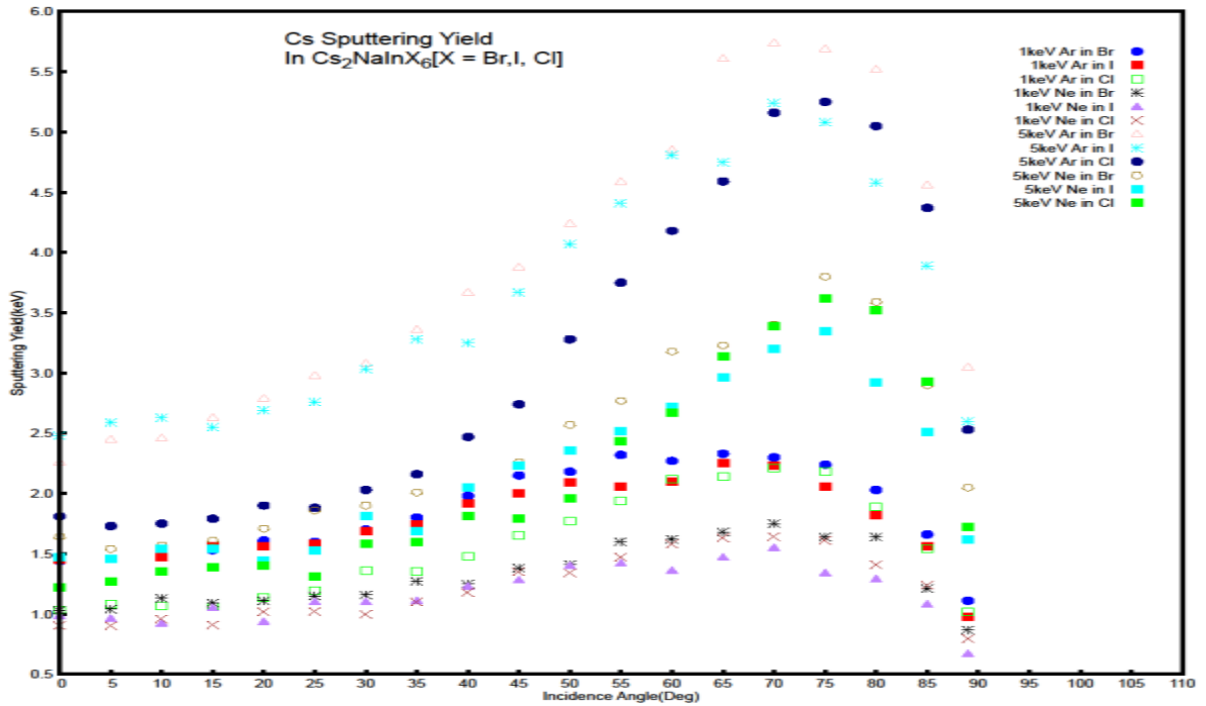


**Fig.2:** Sputter yield of Cs (atoms/ion) for the ejection of Cs atoms from  $Ar^+$  and  $Ne^+$  bombardment of the double perovskites at different angles of incidence, for ion energy of 1keV and 5keV.

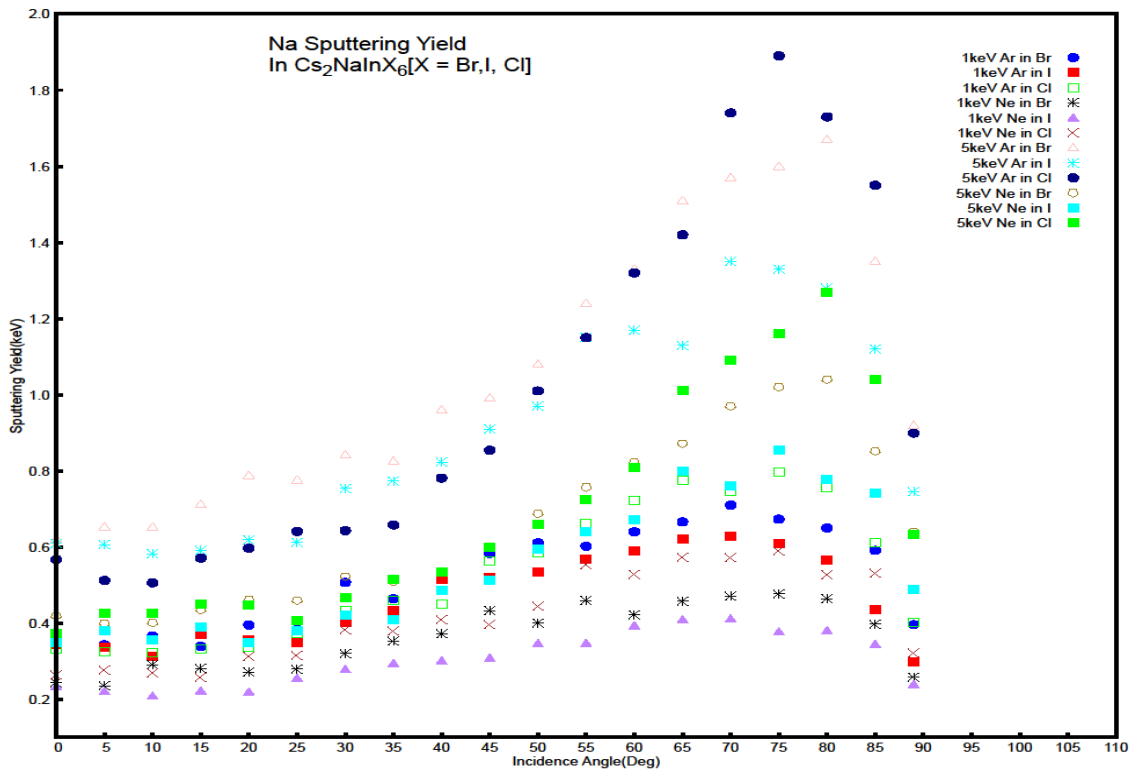


**Fig.3:** Sputter yield of Na (atoms/ion) for the ejection of Na atoms from  $Ar^+$  and  $Ne^+$  bombardment of the double perovskites at different angles of incidence, for ion energy of 1keV and 5keV.

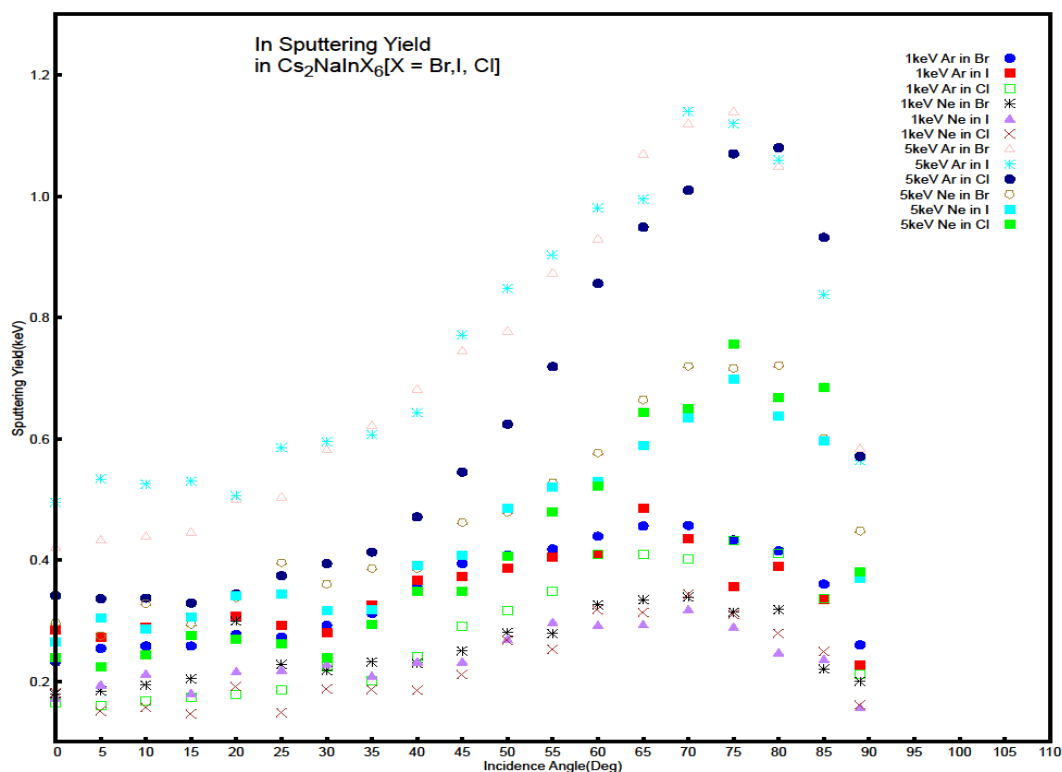


**Fig.4: Sputter yield of In (atoms/ion) for the ejection of In atoms from  $Ar^+$  and  $Ne^+$  bombardment of the double perovskites at different angles of incidence, for ion energy of 1keV and 5keV.**

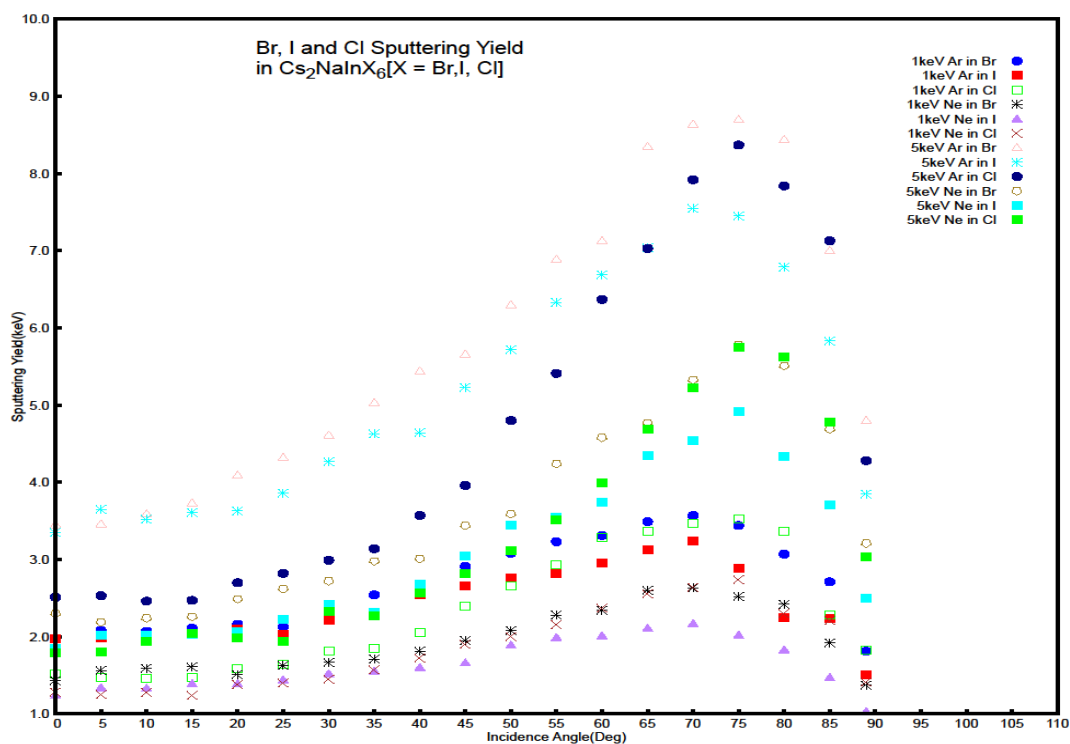


**Fig.5: Sputter yield of Br/I/Cl (atoms/ion) for the ejection of Br atoms from  $Ar^+$  and  $Ne^+$  bombardment of the double perovskites at different angles of incidence, for ion energy of 1keV and 5keV.**

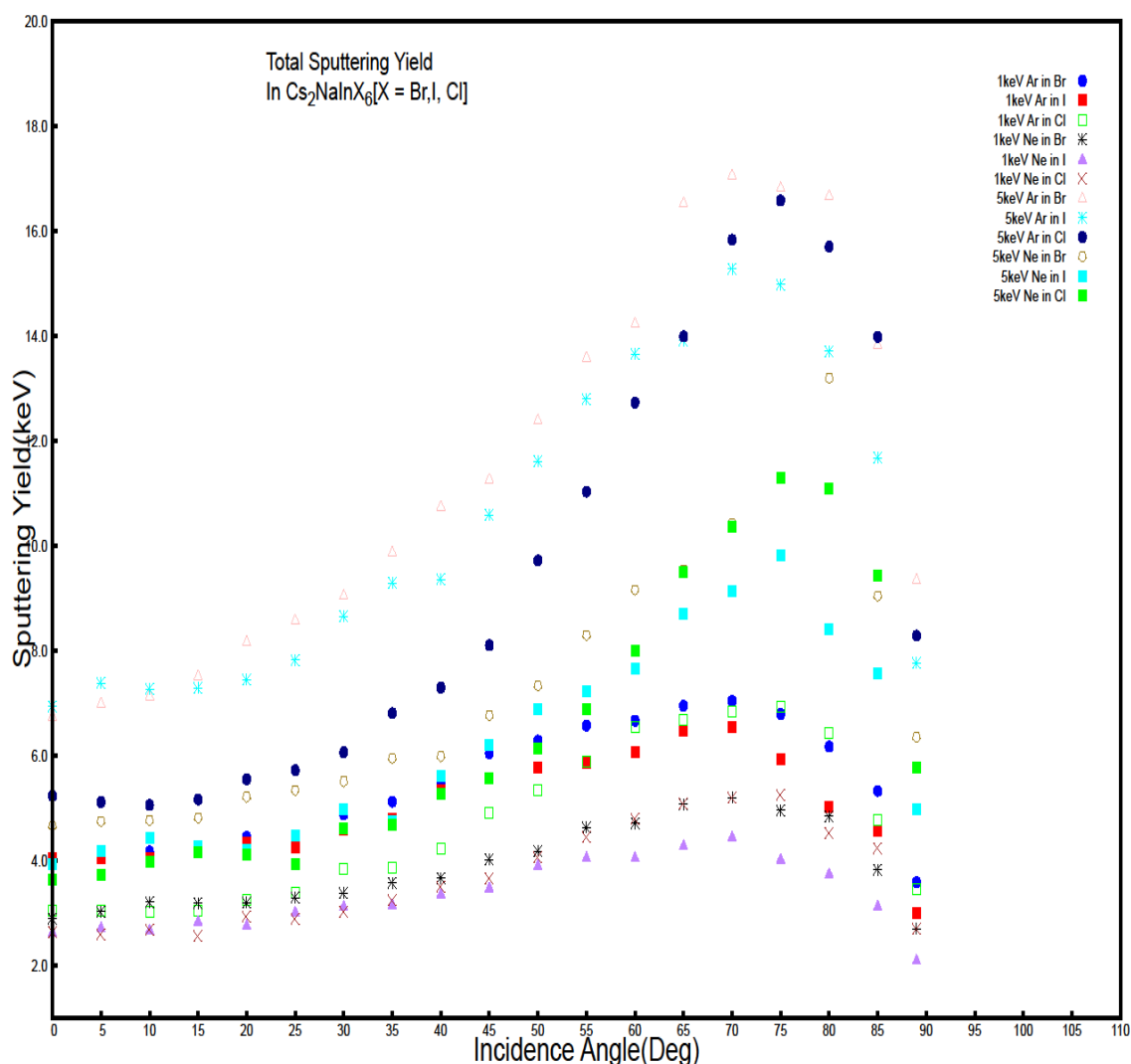


**Fig.6: Sputter yield of CsNaInBr for the ejection of CsNaInBr from Ar<sup>+</sup> and Ne<sup>+</sup> bombardment at different angles of incidence, for ion energy of 1keV and 5keV**

The sputter yield of Cs atoms ranged from 0.67 to 2.32 atoms/ion for 1 keV, and from 1.22 to 5.74 atoms/ion for 5 keV, as shown in Fig.2. Fig.3 shows the yield of Na atoms, which ranged from 0.208 to 0.797 atoms/ion at 1 keV, and from 0.349 to 1.89 atoms/ion at 5 keV. The sputter yields for In atoms, as presented in Fig.4, was the lowest among the constituent elements, ranging from 0.148 to 0.486 atoms/ion at 1 keV and from 0.224 to 1.14 atoms/ion at 5 keV. In contrast, the halide atoms Cl, Br, and I exhibited the highest sputter yields overall, with values ranging from 1.24 to 3.57 atoms/ion at 1 keV, and from 1.79 to 8.7 atoms/ion at 5 keV, as depicted in Fig5. Thus, the order of maximum sputter yields, from lowest to highest, was: In < Na < Cs < X (Cl/Br/I). This ordering reflects the variation in atomic mass, surface exposure, and bond strength of the constituent atoms in the lattice.

Fig.6 presents the total sputter yield behavior for the combined CsNaInX<sub>6</sub> units, at different incidence angles and ion energies. These composite sputter results show the cumulative yield trends and further confirm that sputter yield increased with both ion energy and incidence angle. A peak yield was observed around 78°, consistent across all halide compositions and for both Ne<sup>+</sup> and Ar<sup>+</sup> ions. This again reinforces the angular dependence of sputtering reported in earlier studies.

The higher sputter yield observed for halide atoms compared to Cs, Na, and In can be attributed to their relatively lower surface binding energies and lattice coordination environment. Halide atoms occupy the X-sites of the perovskite framework and are more weakly bound compared to the B-site cation  $\text{In}^{3+}$ , which is octahedrally coordinated within the lattice. The lower sputter yield of indium is consistent with its higher atomic mass and stronger bonding within the crystal structure, requiring greater energy transfer for displacement.

Furthermore, the enhanced sputter yield of  $\text{Ar}^+$  compared to  $\text{Ne}^+$  is consistent with the greater nuclear stopping power of heavier ions, which transfer momentum more efficiently during collision cascades. This leads to shallower penetration depths and higher near-surface energy deposition, thereby increasing sputtering probability.

## CONCLUSION

We performed Monte Carlo simulations of the ion sputtering of  $\text{Cs}_2\text{NaInCl}_6$ ,  $\text{Cs}_2\text{NaInBr}_6$ , and  $\text{Cs}_2\text{NaInI}_6$  (cesium-based double perovskites) as a new perspective for understanding and improving upon the desired physical properties of less toxic metal halide perovskite materials that are based on the possible substitutes for lead. In our studies, reported in this paper, we found the sputtering results of the three halide-based double perovskites chloride, bromide, and iodide to be very similar. In fact, so similar as to serve as another reason why the quest to improve upon the properties of  $\text{Cs}_2\text{NaInX}_6$  materials, especially for photovoltaic applications, should not be abandoned.

The simulation results, which showed consistent trends in ion range, angular dependence, and sputter yields across the different halide compositions, support the view that compositional tuning of the halide site (from  $\text{I}^-$  to  $\text{Br}^-$  or  $\text{Cl}^-$ ) does not significantly alter the fundamental sputtering behavior of these compounds. The sputter yield followed a predictable angular trend, peaking between  $70^\circ$  and  $82^\circ$ , which aligns with previously reported sputtering characteristics for perovskite materials. Among the constituent atoms, the halides were the most easily sputtered, while In showed the lowest yield. These observations further support the structural and energetic stability of these materials under energetic particle irradiation.

These results suggest that sputtering simulations may provide a valuable predictive tool in evaluating the optoelectronic potential of emerging perovskite materials, and that  $\text{Cs}_2\text{NaInX}_6$  compounds deserve further research attention in the ongoing search for high-performance, lead-free alternatives in solar energy applications.

## REFERENCES

- [1] Anders, A. (2000). Ion-induced surface modification and thin film growth. *Surface and Coatings Technology*, 133–134, 78–90. [https://doi.org/10.1016/S0257-8972\(00\)00920-4](https://doi.org/10.1016/S0257-8972(00)00920-4)
- [2] Basavarajappa, M. G., and Chakraborty, S. (2022). Rationalization of double perovskite oxides as energy materials: A theoretical insight from electronic and optical properties. *ACS Materials Au*, 2(6), <https://doi.org/>
- [3] Bradley, R. M., & Harper, J. M. E. (1988). Theory of ripple topography induced by ion bombardment. *Journal of Vacuum Science & Technology A*, 6(4), 2390–2395.

- [4] Cuerno, R., & Barabási, A. L. (1995). Dynamic scaling of ion-sputtered surfaces. *Physical Review Letters*, 74(23), 4746–4749.
- [5] Greul, E., Petrus, M. L., Binek, A., Docampo, P., & Bein, T. (2017). Highly stable, phase-pure Cs<sub>2</sub>AgBiBr<sub>6</sub> double perovskite thin films for optoelectronic applications. *Journal of Materials Chemistry A*, 5(39), 19972–19981. <https://doi.org/10.1039/C7TA05042H>
- [6] J. Ziegler, M. Ziegler, J. Biersack, The stopping and range of ions in matter, *Nucl. Instrum. Meth. Phys. Res. B* 268 (2010) 1818–1823.
- [7] Mahajan, S. (2000). Ion beam processing of materials and devices. *MRS Bulletin*, 25(9), 37–42. <https://doi.org/10.1557/mrs2000.170>
- [8] Maughan, A. E., Ganose, A. M., Bordelon, M. M., Miller, E. M., Scanlon, D. O., & Neilson, J. R. (2018). Tolerance to defects and deviation from stoichiometry in the lead-free halide double perovskite Cs<sub>2</sub>NaInCl<sub>6</sub>. *Chemistry of Materials*, 30(15), 472–483. <https://doi.org/10.1021/acs.chemmater.7b05050>
- [9] McMeekin, D. P., Sadoughi, G., Rehman, W., Eperon, G. E., Saliba, M., Horantner, M. T.... and Snaith, H. J. (2016). A mixed-cation lead mixed-halide perovskite absorber for tandem solar cells. *Science*, 351(6269), 151-155. DOI: 10.1126/science.aad5845
- [10] Oyewande, OE (2025). Title. Seminar held on 22 April, Department of Physics and Engineering Physics, Obafemi Awolowo University. Available online: [www.sci.ui.edu.ng/oyewande](http://www.sci.ui.edu.ng/oyewande).
- [11] Oyewande, O. E., & Akinpelu, A. (2018). An ion-beam surface sputtering approach to the quest for lead-free metal halide perovskite for solar cells. *Nuclear Instruments and Methods in Physics Research Section B: Beam Interactions with Materials and Atoms*, 434, 102–108. <https://doi.org/10.1016/j.nimb.2018.08.041>
- [12] S. Martinie, T. Saad-Saoud, S. Moindjie, D. Munteanu, J. Autran, Behavioral modelling of SRIM tables for numerical simulation, *Nucl. Instrum. Meth. Phys. Res. B* 322 (2014) 2–6
- [13] Sigmund, P. (1969). Theory of sputtering. *Physical Review*, 184(2), 383–416.
- [14] Sigmund, P. (1981). Sputtering by ion bombardment: theoretical concepts. In R. Behrisch (Ed.), *Sputtering by Particle Bombardment I* (pp. 9–71). Springer. [https://doi.org/10.1007/978-3-642-66782-8\\_2](https://doi.org/10.1007/978-3-642-66782-8_2)

- [15] Slavney, A. H., Hu, T., Lindenberg, A. M., & Karunadasa, H. I. (2016). A Bismuth-Halide Double Perovskite with Long Carrier Recombination Lifetime for Photovoltaic Applications. *Inorganic Chemistry*, 55(1), 64–68. <https://doi.org/10.1021/acs.inorgchem.5b02032>
- [16] Slavney, A. H., Hu, T., Lindenberg, A. M., & Karunadasa, H. I. (2017). A Bismuth-Halide Double Perovskite with Long Carrier Recombination Lifetime for Photovoltaic Applications. *Inorganic Chemistry*, 56(1), 46–55. <https://doi.org/10.1021/acs.inorgchem.6b01336>
- [17] W. Wilson, L. Haggmark, J. Biersack, Calculations of nuclear stopping, ranges, and straggling in the low-energy region, *Phys. Rev. B* 15 (1997) 2458.
- [18] Xiao, Z., & Zuo, C. (2020). Design criteria for elpasolite double perovskites for optoelectronic applications. *Nature Reviews Materials*, 5, 416–430. <https://doi.org/10.1038/s41578-020-0190-4>
- [19] Ziegler, J. F., Biersack, J. P., & Littmark, U. (1985). *The Stopping and Range of Ions in Solids*. Pergamon Press.
- [20] Ziegler, J. F., Ziegler, M. D., & Biersack, J. P. (2010). SRIM – The stopping and range of ions in matter (2010). *Nuclear Instruments and Methods in Physics Research Section B: Beam Interactions with Materials and Atoms*, 268(11–12), 1818–1823. <https://doi.org/10.1016/j.nimb.2010.02.091>